Granular Matter (2005) 7: 69–81
DOI 10.1007/s10035-005-0198-x

ORIGINAL PAPER

Nitin Jain · Julio M. Ottino · Richard M. Lueptow

Regimes of segregation and mixing in combined size and density granular systems: an experimental study

Received: 18 May 2004 / Published online: 10 March 2005
© Springer-Verlag 2005

Abstract Granular segregation in a rotating tumbler occurs due to differences in either particle size or density, which are often varied individually while the other is held constant. Both cases present theoretical challenges; even more challenging, however, is the case where density and size segregation may compete or reinforce each other. The number of studies addressing this situation is small. Here we present an experimental study of how the combination of size and density of the granular material affects mixing and segregation. Digital images are obtained of experiments performed in a half-filled quasi-2D circular tumbler using a bi-disperse mixture of equal volumes of different sizes of steel and glass beads. For particle size and density combinations where percolation and buoyancy both contribute to segregation, either radial streaks or a "classical" core can occur, depending on the particle size ratio. For particle combinations where percolation and buoyancy oppose one another, there is a transition between a core composed of denser beads to a core composed of smaller beads. Mixing can be achieved instead of segregation if the denser beads are also bigger and if the ratio of particle size is greater than the ratio of particle density. Temporal evolution of these segregated patterns is quantified in terms of a "segregation index" (based on the area of the segregated pattern) and a "shape index" (based on the area and perimeter of the segregated pattern).

Keywords Granular flow · Granular materials · Mixing Segregation · Organization

N. Jain · J. M. Ottino
Department of Chemical and Biological Engineering,
Northwestern University,
Evanston, IL 60208

J. M. Ottino · R. M. Lueptow (✉)
Department of Mechanical Engineering,
Northwestern University,
Evanston, IL 60208
E-mail: r-lueptow@northwestern.edu
Tel.: +847-491-4265

1 Introduction

Examples of flow-driven mixing and segregation of granular materials range from industrial applications such as rotating kilns and industrial tumblers to natural phenomena such as avalanches and transport in riverbeds. The basic mechanisms are imperfectly understood. However, over the last fifty years, there have been a number of attempts to understand the flow, handling, and characterization of granular materials [1–4] and considerably more is known now about granular flow physics than just a decade ago (for summaries of recent work, see [5–7]). Despite these efforts, the understanding of granular flow and mixing is still far less advanced than that for fluid mixing [8]. One complicating characteristic of granular flow is that granular materials that differ in size or density tend to segregate. For instance, if a container filled with two different types of granular materials is shaken, larger grains migrate to the top of the container, a phenomenon called the "Brazil nut" effect [9]. The other complication is that it is hard to come up with fool-proof rules about segregation; seemingly every rule is bound to have exceptions [10]. Even the most celebrated segregation mechanism, the Brazil nut effect, has an opposite – depending on the density, the larger grains can either rise to the top or sink in a shaken granular bed [11, 12].

Two special cases of granular segregation have received the most attention – S-systems where particles of the same density differ in size; and D-systems where particles of the same size differ in density. Nearly all studies to date have been restricted to binary systems. Both cases present theoretical challenges [13] with the case of S-systems presenting the most serious problems. As might be imagined, even more challenging is the case where density and size segregation may compete or reinforce each other. This case is of clear practical importance. Granular flows in industry and nature often involve particles that differ in both size and density. In these situations, several questions arise: (1) What particle size and density combinations result in mixing instead of segregation? (2) When is segregation dominated by size and when is it dominated by density? (3) How does the segregation pattern depend on particle properties? However, the

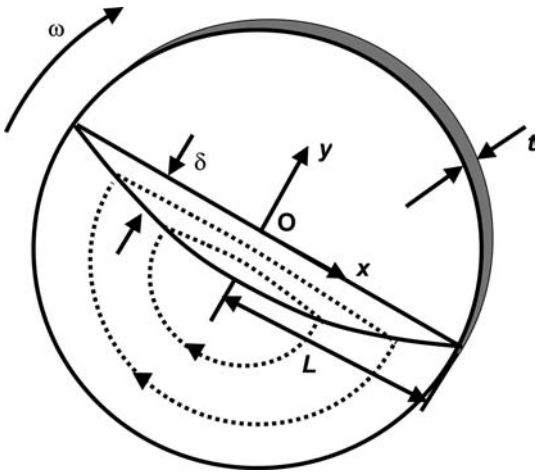

Fig. 1 Schematic of rotating tumbler geometry with the coordinate system and the system parameters

number of studies addressing this situation is small. Here we present an experimental study of how the combination of size and density of the granular material affects mixing and segregation and organize the results in terms of a phase portrait whose axes are the density ratio and the size ratio. We hope that the results may spur theoretical analysis of this important process.

We study the process in a quasi two-dimensional tumbler of circular cross-section that is half filled with granular material and is rotated about its horizontal axis to produce a circulating flow, as shown in Fig. 1. We restrict our investigations to non-cohesive dry beads. The beads flow along the sloped surface due to gravity in a narrow lens-shaped surface layer of thickness δ. The remainder of the material rotates as a solid body until it reaches the flowing layer. Depending on the speed of rotation, different flow regimes can occur – avalanching, rolling or cascading, cataracting, and centrifuging [14, 15]. This paper focuses on the rolling regime, in which the flow is continuous and the upper surface of the flowing layer is nearly flat.

When the particles are mono-disperse, tumbling over several revolutions results in mixing. However, a difference in particle size or density leads to segregation instead of mixing [16]. If particles differ in size, known as an "S-system", upon flow, the smaller particles fall through the interstices between the larger particles to lower levels in the flowing layer as shown schematically in Fig. 2a. This mechanism is called *"percolation"*. On the other hand, if the particles differ in density, known as a "D-system," the heavier particles sink to lower levels in the flowing layer while lighter ones rise as shown in Fig. 2b. This mechanism is called *"buoyancy"*. As these mechanisms continue to operate in a rotating tumbler, smaller or denser particles fall out of the flowing layer and deposit near the middle of the fixed bed as a segregated core, a process known as radial segregation. Radial segregation is quite fast – it is readily evident within 1 to 2 rotations [17–19].

The purpose of this study is to determine how the combination of size and density of the granular material affects granular segregation. Granular materials of higher density or smaller size tend to radially segregate at the core of the granular bed while granular materials of lower density or larger size tend to segregate at the outer edges of the granular bed and in the flowing layer. Of course, it seems likely that if the mixture consists of small-heavy beads and large-light beads, the smaller beads will sink to lower levels in the flowing layer ending up in the segregated core because of both *"percolation"* and *"buoyancy"* (Fig. 2c). One would expect that in this case, the rate at which segregation occurs and/or the extent of final segregation would be greater than the cases when only size or density of the particles drives the segregation. Conversely, for large-heavy particles and small-light particles, one might expect that segregation could be minimized or even eliminated altogether because the percolation and buoyancy mechanisms oppose one another (Fig. 2d).

A significant amount of experimental and computational research has been done to study segregation in rotating tumblers. In most of these studies bi-disperse particles differ in only one property – either size (S-system) or density (D-system). For instance, Nityanand et al. [17] observed smaller particles moving to the core of the bed for the cascading regime, presumably due to percolation. Clement et al. [18] and Cantalaube and Bideau [19] found that a single intruder particle that is smaller than the bulk moved toward the core region, while an intruder that is larger than the bulk moved close to the periphery of the tumbler. Particle percolation explains both cases. Thomas [10] considered how the relative concentration of beads of different sizes but the same density affects segregation. At a lower size ratio, geometrical effects (percolation) force the larger beads to the free surface. As a result, these beads are located close to the periphery of the tumbler when entrapped in the fixed bed. As the size ratio is increased, the mass of the larger beads becomes important and opposes these geometrical effects. At size ratios greater than 5, a segregation reversal takes place with larger beads sinking into the core while the smaller beads are located at the periphery of the tumbler.

On the computational front, both continuum models and particle dynamic simulations have been developed separately for size and density segregation. Khakhar et al. [20] performed experiments and developed a continuum model to explain radial segregation for D-systems based on an "effective" buoyancy and a Lagrangian approach to obtain the dynamic evolution of the concentration distribution. Later, Khakhar et al. [21] developed a continuum model to explain radial ("classical" core formation) and non-radial segregation patterns for S-systems. Ristow [22] and Dury & Ristow [23] used particle dynamics simulations to analyze segregation in D-systems and S-systems. Prigozhin and Kalman [24] developed a model for both the rolling and avalanching regimes for S-systems using the experimental data of Drahun and Bridgwater [25] and devised a material-independent mass transfer model. In all cases, only the size or the density of the particles differed, so either percolation or buoyancy provide a satisfactory explanation for the radial segregation.

In only a few studies are both the size *and* density of granular particles varied simultaneously (SD-system). Drahun

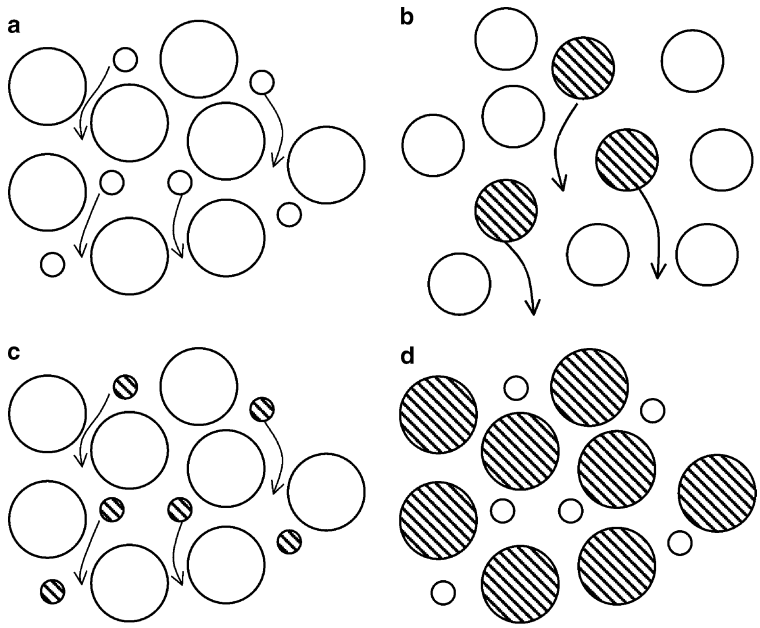

Fig. 2 Segregation mechanisms. (a) segregation driven by percolation only; (b) segregation driven by buoyancy only; (c) segregation when percolation and buoyancy act together; and (d) segregation when percolation and buoyancy oppose each other. Symbol fill: open – lower density particles; filled – higher density particles

and Bridgwater [25] performed free segregation experiments on an inclined plane in which small amounts of tracer particles were slowly fed into a bulk of 4 mm glass beads. They observed that percolation and buoyancy offset each other and the segregation was reduced when the size and density of the tracer particles were both lower than the size and density of the glass beads. Alonso et al. [26] performed the first work on a SD-system in a quasi-2D circular tumbler to directly address the competition between buoyancy and percolation. They developed simplified quantitative relations for sinking of denser particles based on the mass of the particles and particle percolation based on the probability of a single particle percolating through a bed of bigger beads. Using combinations of 13 different material types with densities of 1.08 to 7.78 g/cm^3 and particle diameters of 0.7 to 5.0 mm, they showed agreement between the experimentally measured mixing and a theoretical segregation index. More recently, Metcalfe and Shattuck [27] used Magnetic Resonance Imaging (MRI), to study the segregation of a SD-system in a long cylindrical tube. They found that density and size segregation almost cancelled each other for the case of glass beads (2 mm diameter, 2.6 gm/cm^3) and brown mustard seeds (1.4 mm diameter, 1.7 gm/cm^3).

The central purpose of the current work is to consider the competition between percolation and buoyancy. Our study differs from the previous work in a number of ways: (1) We use a broader and better defined size and density range than the previous studies. Glass and steel beads are used so that the density changes by a factor of 3. Five different sizes from 0.2 mm to 4 mm are used for glass beads and four different sizes from 1 mm to 4 mm are used for steel beads; (2) We analyze all 20 combinations of these bead sizes and densities to better understand the impact of changing the size ratio while keeping the density ratio fixed; (3) We obtain digital images of the system to non-invasively measure the temporal evolution of segregation and record the segregation pattern in the quasi-2D tumbler.

2 Experimental procedure

It is important to point out at the outset that even though the experiment is relatively simple, the number of parameters is large: the speed of rotation, the properties of the interstitial fluid [28], the fill fraction (half-full, more or less than half-full), the flow regime (avalanching, rolling, etc), the cross-sectional shape of the tumbler (circular or non-circular), the particle properties (size and density of granular materials), the relative concentration of the two types of particles, and the friction between granular material and the cylinder walls. In order to limit the scope of the work, we focus only on the particle properties. All the experiments involve dry granular materials in the rolling regime. Most experiments are performed with a fill fraction of 50%, although a limited number of experiments are done for other fill fractions to explore the sensitivity of the segregation to the fill fraction.

The circular tumbler used in the quasi-2D experiments is shown schematically in Fig. 1. The tumbler is 28 cm in diameter (D). The front faceplate of the tumbler is clear acrylic to permit optical access. The back surface of the tumbler is also made of clear acrylic to ensure similar conditions on both ends of the tumbler. A stepper motor and micro series driver combination (SLO-SYN®) is used to rotate the tumbler at

rotational speed (ω) of 0.21 rad/s (2 rpm), corresponding to Froude number, $Fr = \omega^2 L/g$ of about 6.3×10^{-4}, where L is the half-length of the flowing layer (0.5 D for a half-filled tumbler). A limited number of experiments are performed at rotational speeds of 0.105 rad/s (1 rpm), 0.42 rad/s (4 rpm), 0.84 rad/s (8 rpm), and 1.68 rad/s (16 rpm) to determine the sensitivity to rotational speed.

Spherical chrome steel beads (7.5 g/cm^3 d_s = 1 to 4 mm in diameter) and glass beads (2.5 g/cm^3 d_g = 0.2 to 4 mm in diameter, Fox Industries) are used for experiments. The ratio of the tumbler radius to bead diameter is 35 to 700. In all experiments, the dimensionless axial length of the tumbler, t, is set to 3.2 times the diameter of the bigger beads in order to maintain similarity with respect to particle diameter. The use of quasi two-dimensional tumbler is a balancing act of sorts. Too small of an axial length amplifies wall friction effects. Increasing the thickness, however, brings complications as axial segregation starts playing a role [29].

Experiments are conducted using 50/50 volume fraction of steel and glass beads. Beads are initially well mixed. Images are obtained with a TSI® charge-coupled device camera for the initial condition and every 1/8th rotation thereafter to permit analysis of the temporal development of mixing or segregation. Twenty different experiments are performed using various combinations of steel and glass beads. The matrix of experiments is shown in Fig. 3. The shaded cells along the diagonal represent the cases for which the size of the steel and glass beads is the same. Below this diagonal line, the steel beads are smaller than the glass beads ($0.25 \leq d_s/d_g \leq 0.75$). The notation "S + D" indicates that percolation based on size (S) and buoyancy based on density (D) act in the same direction, as shown in Fig. 2(c). Above the diagonal the steel beads are larger than the glass beads ($1.33 \leq d_s/d_g \leq 20$). The "S − D" notation indicates percolation and buoyancy oppose one another. After each experiment steel and glass beads are separated with a magnet. After separating the beads, the steel beads are demagnetized.

GLASS \ STEEL	1 mm	2 mm	3 mm	4 mm
0.2 mm	S-D	S-D	S-D	S-D
1 mm	D	S-D	S-D	S-D
2 mm	S+D	D	S-D	S-D
3 mm	S+D	S+D	D	S-D
4 mm	S+D	S+D	S+D	D

Fig. 3 Matrix of experiments performed. "D" represents experiments with particles of the same size but different density. "S+D" are experiments for which steel beads are smaller than glass beads, so percolation and buoyancy act together. "S−D" are experiments for which steel beads are larger than glass beads, so that percolation and buoyancy oppose each other

3 Results

Initial tests are performed for a D-system, along the diagonal in Fig. 3, where particles are of the same size but differ in density. Consistent with previous results for buoyancy-driven segregation [20,30] the radial granular segregation is very fast – a segregated pattern is formed in only 1 to 2 rotations. Within 5 rotations segregation pattern is complete and reaches a steady state. Of course, heavier beads (steel) segregate in the semicircular core while lighter beads (glass) remain at the periphery of the tumbler – the "classic" segregation pattern.

A more complicated situation occurs when both "buoyancy" and "percolation" act in the same direction – the area below the diagonal in the experimental matrix (Fig. 3). Figure 4 shows the segregation patterns after 20 revolutions for 1 mm steel beads (darker areas) and glass beads ranging from 2 mm to 4 mm in diameter. In all cases the beads segregate. But for ratios of the steel bead diameter to the glass bead diameter (d_s/d_g) of 1/2 and 1/3, radial streaks form rather than the "classical" core. The segregation pattern in the first few rotations begins as a classical core, similar to that for equal size beads ($d_s/d_g = 1$). As time progresses, the radial streaks form.

The formation of similar radial streaks was first reported by Hill et al. [30] for a square tumbler. They performed experiments involving 0.8 and 2.0 mm glass beads in the rolling regime and radial streaks were observed at a fill fraction of just over 50%, though not for a half-full tumbler. This study was followed by a detailed experimental and computational work by Khakhar et al. [21]. They observed streak formation in a circular tumbler for all possible combinations involving 1 mm, 2 mm, and 3 mm glass beads. Most of their experimental work was at a fill level of 50%. At a fill level of 25%, they found that the radial streaks disappeared. Irrespective of the shape of the tumbler, both of these studies suggested that streaks occur when there is a sufficiently large difference in particle size that leads to higher "fluidity" of the smaller beads relative to the larger beads. "Fluidity" can be explained using mass balance arguments. The mass flow rate of granular materials in the flowing layer (of thickness δ) must equal the mass flow rate in the fixed bed, resulting in the velocity of granular material at the flowing surface scaling inversely with δ [31,32]. The flowing layer is thicker for larger beads compared to smaller beads [31] resulting in higher "fluidity" of the smaller beads than the larger beads. However, the concept of "fluidity" has been qualitative to date.

In order to quantify the "fluidity" we measure the velocity of the 1 mm steel and 2 mm glass beads using a combination of Particle Image Velocimetry (PIV) and Particle Tracking Velocimetry (PTV). The clear side of the tumbler is illuminated by dual-YAG laser passing through a diffuser

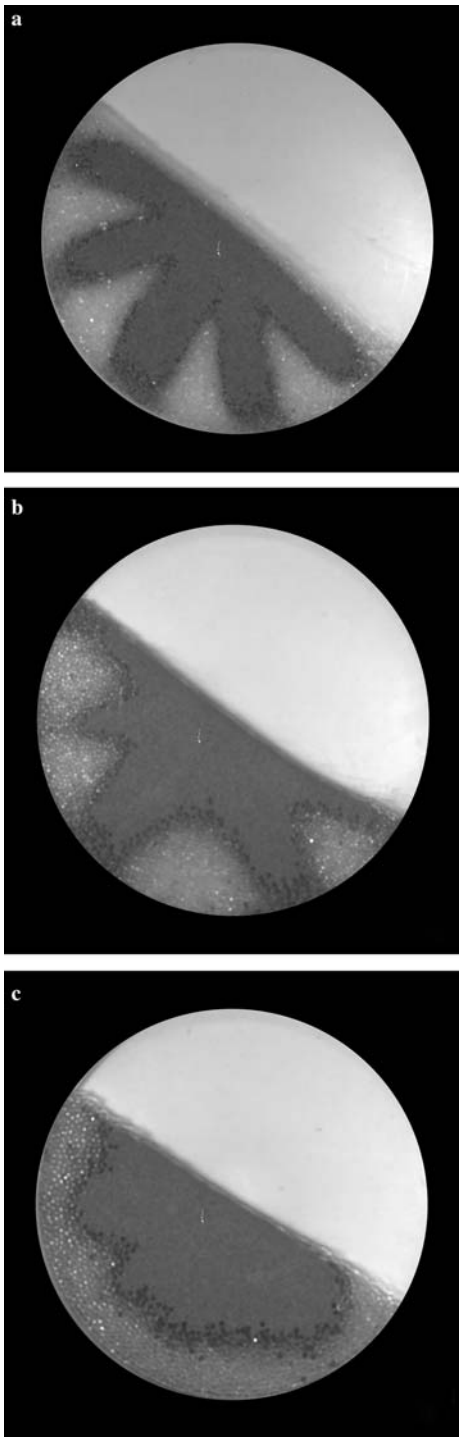

Fig. 4 Segregation patterns when buoyancy and percolation mechanisms act in the same direction ("S+D"). 1 mm steel beads tumbled with (a) 2 mm glass beads ($d_s/d_g = 0.5$); (b) 3 mm glass beads ($d_s/d_g = 0.33$); and (c) 4 mm glass beads ($d_s/d_g = 0.25$)

plate to generate a flash of light. The light reflected back from the particles in the tumbler is recorded by a standard PIV system having a CCD camera with a resolution of 1016 × 1000

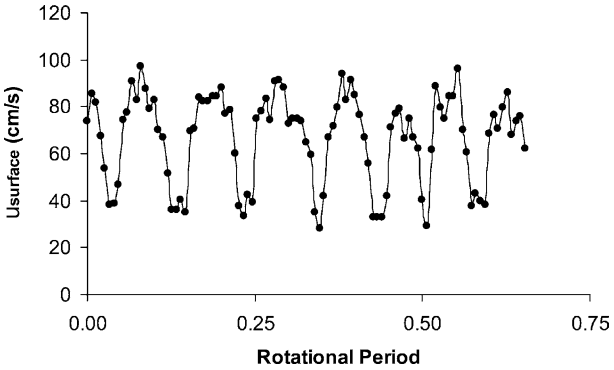

Fig. 5 Maximum surface velocity in the flowing layer for a bi-disperse system of 1 mm steel and 2 mm glass beads ($d_s/d_g = 0.5$) as a function of the rotational period of the tumbler. The tumbler is rotated at an angular velocity of 2 rpm (0.21 rad/s). Images of the flow (not shown) indicate a high concentration of glass beads in the flowing layer corresponding to surface velocity of about 40 cm/s and a high concentration of steel beads in the flowing layer corresponding to surface velocity of about 90 cm/s

pixels. The camera's field of view is zoomed in on the center of lens shaped flowing layer (Fig. 1) to capture a region about 2 cm square. The PIV system (TSI. Inc.) synchronizes the camera, laser flashes, and frame grabber to obtain a pair of images separated by a small time delay (1000 μs) at a frequency of 5 Hz. PIV is used to estimate the velocity of particles on a statistically averaged basis, followed by PTV to find the particle velocity on a particle-by-particle basis similar to our previous work [32].

Figure 5 shows the maximum velocity at the surface of the flowing layer for 99 image pairs with each pair separated by 0.2 sec. The experimental images are acquired after approximately 20 rotations when radial streaks are fully developed. As is evident in Fig. 5, the maximum velocity at the flowing surface varies from 40 cm/s to 90 cm/s. From the images of the flow (not shown), it is clear that the velocity of about 40 cm/s corresponds to the case when the flowing layer is predominantly large glass beads and the velocity of about 90 cm/s corresponds to when the layer contains mostly small steel beads, which form the streaks evident in Fig. 4. The maximum and minimum velocities are similar to the velocities reported in our previous work for different sized monodisperse steel beads in a tumbler of same dimensions [31]. Segregation in the first couple of rotations begins as a "classical core" with the small beads in the lower half of the flowing layer and in the segregated core. As core formation nears completion, the smaller beads, which travel twice as fast as the larger beads in the flowing layer, are able to reach the end of the flowing layer before sinking to lower levels in the flowing layer resulting in a small radial streak. The streak continues to grow and lengthen upon reentry of the smaller beads that had previously reached the periphery of the tumbler into the flowing layer. The process of streak growth continues for about 10 revolutions until a stable streak segregation pattern is formed.

Hill et al. [30] and Khakhar et al. [21] showed that streak formation occurs in S-systems. Furthermore, streaks have not

been observed in D-systems. Thus, the appearance of streaks for SD-systems seems to be related to size segregation rather than density segregation for $d_s/d_g < 1$. However, as the particle diameter ratio is reduced further to $d_s/d_g = 0.25$ (Fig. 4c), the "classical" segregation pattern reappears instead of even more prominent streaks that might be expected based on the work of Khakhar et al. [21]. Clearly there appears to be both an upper bound and a lower bound on d_s/d_g for radial streaks to appear. Most likely, as the size ratio is decreased, percolation in the flowing layer becomes stronger. Small beads with greater "fluidity" in the flowing layer are no longer able to reach the periphery of the tumbler, because they quickly percolate to lower levels in the flowing layer. The result is the disappearance of radial streaks for small particle diameter ratios.

Similar results to those described above are observed for steel beads larger than 1 mm as long as they are smaller than the glass beads. Radial streaks form for the combination of 2 mm steel and 3 mm glass beads (Fig. 6a), although the streaks do not reach the periphery of the tumbler and are not as prominent as those for 1 mm steel beads. A similar result was observed by Khakhar et al. [21] for the S-system of 2 mm and 3 mm glass beads. For the remaining combinations −2 and 3 mm steel beads tumbled with 4 mm glass beads – the "classical" segregation pattern occurs instead of radial streaks (Fig. 6b and 6c). This leads to the question of why streaks do not occur for 2 mm steel and 4 mm glass beads when they occur for the identical size ratio of 1 mm steel and 2 mm glass beads. Most likely, 2 mm steel beads are less "fluid" than the 1 mm steel beads. The reduced "fluidity" of the larger steel beads causes them to sink toward the core before traversing the length of the flowing layer, therefore, preventing streak formation. Particles sinking into the flowing layer due to the combination of percolation and buoyancy has a greater impact than the fluidity of the smaller beads preventing streak formation for 2 and 3 mm steel beads tumbled with 4 mm glass beads.

A very different situation occurs above the diagonal in the matrix of Fig. 3 ($d_s/d_g > 1$), where there is a competition between the "buoyancy" and "percolation" mechanisms. The large steel beads tend to sink toward the center of the tumbler due to buoyancy while the small glass beads tend to fall toward the center due to percolation. Figure 7 shows the steady state segregation patterns after 20 rotations for the case of 4 mm steel beads and different sized glass beads ranging from 0.2 mm in diameter to 3.0 mm in diameter. The 0.2 mm glass beads and 4.0 mm steel beads ($d_s/d_g = 20$) remain mixed, suggesting that buoyancy and percolation balance each other. Extending the experiment for long times (up to 100 rotations) or higher angular velocities (up to 16 rpm) does not alter the final steady state pattern shown in Fig. 7a.

Increasing the diameter of glass beads to 1.0 mm results in a slight tendency toward segregation with a higher concentration of steel beads at the periphery (Fig. 7b). Small glass beads are mixed with the large steel beads at the periphery and the segregation is incomplete. The presence of small glass beads with the large steel beads at the periphery of the tumbler instead of a narrow band of only steel beads could be related to the idea of two localized regions for smaller beads at the inner core and at the periphery of the tumbler [18]. Conversely, one can argue that the glass beads and steel

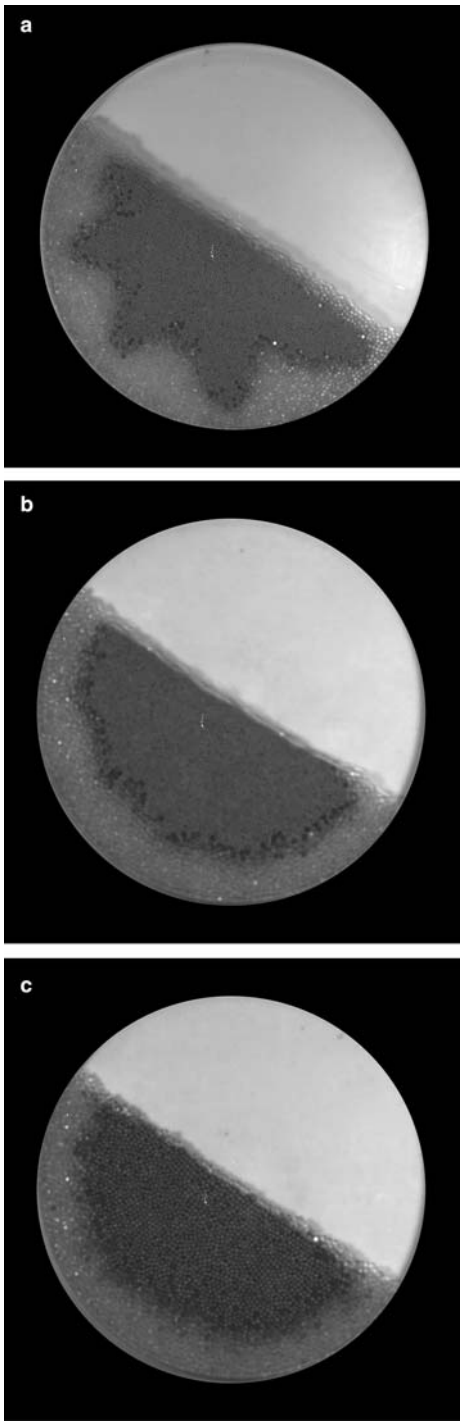

Fig. 6 Segregation patterns when buoyancy and percolation act in the same direction ("S+D"). (a) 2 mm steel beads tumbled with 3 mm glass beads ($d_s/d_g = 0.66$); (b) 2 mm steel beads tumbled with 4 mm glass beads ($d_s/d_g = 0.5$); (c) 3 mm steel beads tumbled with 4 mm glass beads ($d_s/d_g = 0.75$)

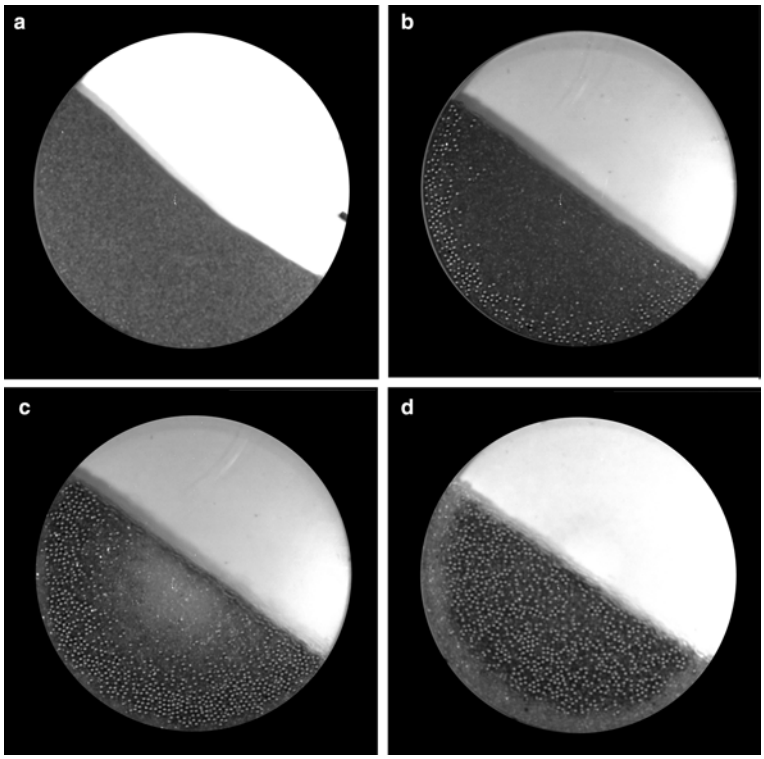

Fig. 7 Segregation patterns when buoyancy and percolation oppose each other ("S−D"). 4 mm steel beads tumbled with (a) 0.2 mm glass beads ($d_s/d_g = 20$) – no segregation; (b) 1 mm glass beads ($d_s/d_g = 4$) – band of high concentration steel beads at the tumbler periphery; (c) 2 mm glass beads ($d_s/d_g = 2$) – small core of glass beads, a band of steel beads, and a band of glass beads at the periphery; and (d) 3 mm glass beads ($d_s/d_g = 1.33$) – core of steel beads

beads are well-mixed throughout the tumbler except for the periphery because of a very slight tendency for percolation. Once again, extending the time of the experiment (up to 100 rotations) or increasing the angular velocity (up to 16 rpm) has no impact on the final pattern. It is reasonable to assume that a higher concentration of steel beads close to the periphery occurs because percolation is slightly more effective than buoyancy, forcing the larger steel beads to be preferentially located close to the periphery. This trend is also evident for the larger 2 mm glass beads ($d_s/d_g = 2$) as shown in Fig. 7c. In this case, the core of smaller glass beads is relatively small because some of the glass beads are also segregated in a narrow band at the periphery of the tumbler outside the band of steel beads. Others are mixed with the steel beads in a band between the periphery and the core. Thus, reducing the size ratio of steel to glass beads weakens the percolation mechanism relative to the buoyancy mechanism. As a result, fewer glass beads segregate in the core and steel beads are evident closer to the center of the bed (Fig. 7c).

As the size of the glass beads is increased to 3 mm, just smaller than the 4 mm steel beads ($d_s/d_g = 4/3$), a core of steel beads forms (heavier particles instead of smaller particles) as shown in Fig. 7d, indicating that at this point buoyancy dominates over percolation. Experiments for other sizes of steel beads yields results similar to those shown in Fig. 7. For 0.2 mm glass beads and 2 or 3 mm steel beads ($d_s/d_g =$ 10 and 15), no segregation is observed, similar to Fig. 7a. Experiments involving 0.2 mm glass beads with 1 mm steel beads ($d_s/d_g = 5$) and 1 mm glass beads with 3 mm steel beads ($d_s/d_g = 3$) produce results similar to Fig. 7b with a thin band of steel beads close to the periphery. For 2 mm steel beads with 1 mm glass beads ($d_s/d_g = 2$) and 3 mm steel beads with 2 mm glass beads ($d_s/d_g = 3/2$), there is a small core of glass beads, a thin band of glass beads at the periphery, and a band of steel beads between the periphery and the core. Reducing the particle size ratio to less than 3/2 produces a result similar to Fig. 7d in which density dominates segregation, and there is a "classical" core of steel beads with glass beads at the periphery.

Figure 8 summarizes the experimental results in the form of a phase plot with the axes of plot being the size of the steel beads and the size of the glass beads. We report six distinct patterns on this plot. For all cases the first part (row) of the symbol stands for the dominant segregation mechanism – percolation/size (S); buoyancy/density (D); or percolation/size combined with buoyancy/density ($S+D$ or $S-D$). The second part (row) of the symbol indicates the final segregation pattern. "*Mixed*" represents the case of mixing instead of segregation, which is observed when the size of steel beads is 10–20 times that of glass beads. An example of the "*mixed*" (no segregation) case is 4 mm steel beads with 0.2 mm glass beads as shown in Fig. 7a. Depending on the relative size

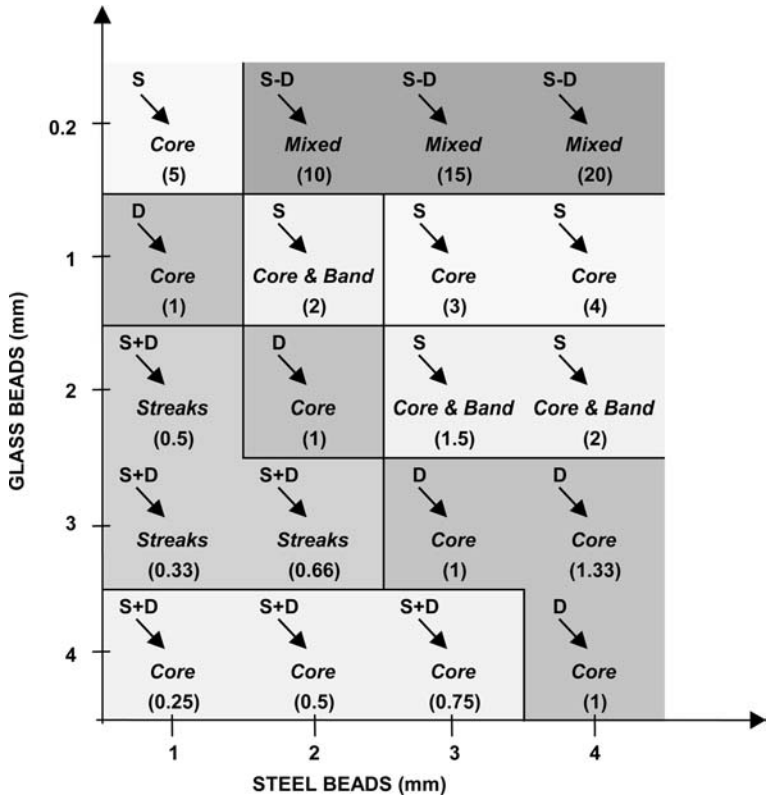

Fig. 8 Phase plot of mixing and segregation. Dominant segregation mechanism: S (percolation or size); D (buoyancy or density); S+D or S−D (percolation and buoyancy). The final segregation pattern is indicated in italics: no segregation *(Mixed)*, a core of glass or steel beads *(Core)*, streaks of steel beads *(Streaks)*, and a core of glass beads with a band of glass beads at the periphery *(Core & Band)*

of steel beads and glass beads (number in the parenthesis in Fig. 8), other segregation patterns appear including a *"Core," "Streaks,"* and the case when glass beads appear in the core as well as in a band near the periphery of the tumbler, *"Core & Band."*

As shown in Fig. 8, classical core segregation is observed in most cases. However, some combinations of small steel and larger glass beads can lead to streaks of steel beads ($S + D \rightarrow Streaks$). Streaks are very sensitive to particle size and occur only for small steel beads that have higher "fluidity" in the flowing layer. Streaks occur for 1 mm steel beads tumbled with 2 or 3 mm glass beads but disappear if the size of glass beads is 1 mm or greater than 3 mm. A classical core composed of higher density beads ($D \rightarrow Core$) occurs when steel beads are either the same size or slightly larger than the glass beads. Smaller glass beads ($S \rightarrow Core$) or smaller steel beads ($S + D \rightarrow Core$) segregate in a classical core for many size combinations. However, when the ratio of particle sizes is $3/2 \leq d_s/d_g \leq 2$, a band of smaller beads appears near the periphery in addition to smaller beads in the core ($S \rightarrow Core\ \&\ Band$). An example of this segregation pattern is the case of 4 mm steel and 2 mm glass beads, shown in Fig. 7c.

All the experiments presented thus far are performed at an angular velocity of 2 rpm. However, previous research on granular segregation indicates that angular velocity can be a key parameter, even reversing the segregation pattern at higher angular velocities [17]. In order to examine this, we perform experiments at different angular velocities for 1 mm steel and 3 mm glass beads (radial streaks), 4 mm steel and 4 mm glass beads ("classical" core formation), 0.2 mm glass and 4.0 mm steel beads (no segregation), and 2 mm glass and 4.0 mm steel beads (steel beads in a band between the core and the periphery). For all of these experiments angular velocity is varied from 1 rpm to 16 rpm. The segregation pattern is sensitive to the angular velocity for the case of radial streaks only, as shown in Fig. 9 for 1, 4, 8, and 16 rpm. The radial streaks are the most prominent for 1 rpm (Fig. 9a) and 2 rpm (Fig. 4b). As the angular velocity is increased to 4 rpm, just as the flow changes from rolling to cataracting, the streaks are fewer, thicker, and do not necessarily reach the periphery of the tumbler. Further increasing the angular velocity to 8 rpm causes the streaks to appear only as bulges in the semi-circular portion of the core. At an angular velocity of 16 rpm segregation still occurs, but the radial streaks are replaced by "classical" core of steel beads.

We also consider the effect of fill fraction on the granular segregation pattern for the same four cases as are used to investigate the effect of angular velocity because previous work has shown that in square tumblers the segregation pattern depends on the fill level [30]. Fill fractions between 40% and 65% are considered while the angular velocity is

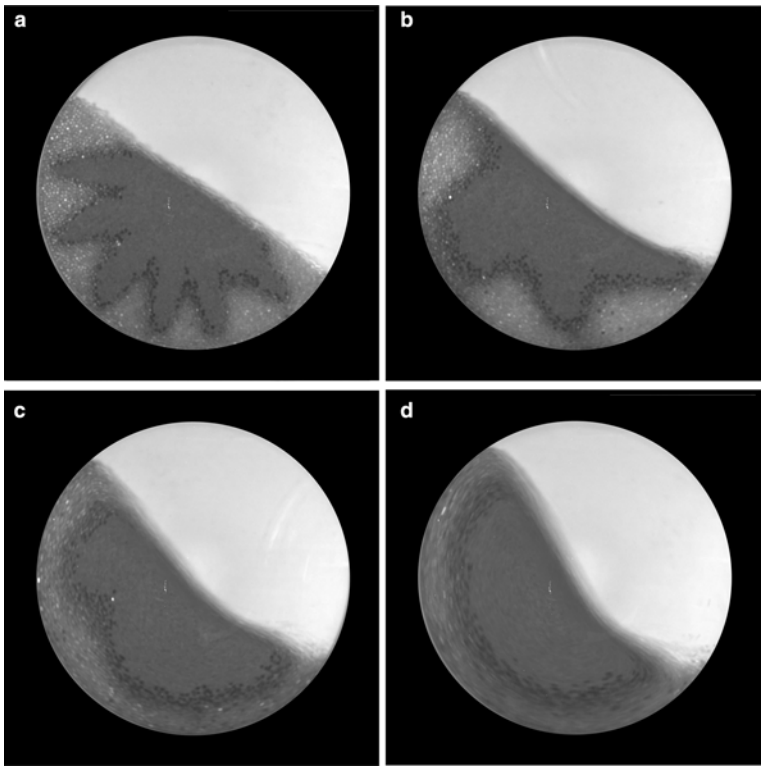

Fig. 9 Effect of angular velocity on granular segregation. Segregation patterns after 20 rotations for 1 mm steel beads and 3 mm glass beads ($d_s/d_g = 0.33$) (a) 1 rpm; (b) 4 rpm; (c) 8 rpm; and (d) 16 rpm

maintained at 2 rpm. The fill fraction is based on a line perpendicular to the flowing layer surface that extends from the center of the flowing layer to the wall of the tumbler. The fill fraction is the ratio of the length of this line to the diameter of the tumbler. For the conditions that result in no segregation, classical core formation, or a band of steel beads between the periphery and the core, there is almost no effect of different fill fractions on the granular segregation. However, for the case where streaks form (1 mm steel and 3 mm glass beads), changes in fill fraction affect the nature of the streak pattern. Figure 10 shows the segregation pattern after 20 rotations for 1 mm steel beads and 3 mm glass beads and for four different fill levels −40%, 48%, 60%, and 65%. Streaks occur for all of these fill fractions. Reducing the fill fraction from 50% (Fig. 4b) to 48% (Fig. 10b) to 40% (Fig. 10a) makes the streaks less prominent so that they do not reach the periphery of the tumbler. Increasing the fill level to 60% makes the streaks quite prominent (Fig. 10c). However, increasing the fill level further to 65% reduces the tendency toward streaks (Fig. 10d). From Fig. 10 it is evident that there is a large range of fill levels at which radial streaks occur. The variation in the degree of streak formation with fill level is probably related to the variation in the flowing layer thickness, velocity, and length. For some conditions such as the 60% fill level (Fig. 10c), the tendency to form streaks due to the fluidity of the steel beads is apparently reinforced by the thickness and length of the flowing layer at that fill level. In other words, the flowing layer structure (thickness and length) at this fill level is such that the fluidity of the steel beads carries the beads to the end of the flowing layer before they sink lower in the flowing layer, thus forming prominent streaks. At both lower and higher fill levels, the reinforcement by the flowing layer structure of the streak formation by fluidity is weaker, so the streaks are less prominent.

Finally, we also consider the effect of friction between granular material and the end walls of the tumbler. Experiments presented thus far were first performed using a brand-new acrylic end-wall and later repeated using the same plate after it had been used to perform the 20 distinct experiments [Fig. 3]. Results are reproducible even though the plate was scratched from the previous experiments, indicating that the segregation patterns depend predominantly on the particle size and density and are relatively independent of the wall friction.

To permit the analysis of the transient character of segregation, digital images of the tumbler are obtained after every 1/8th rotation for each of the conditions at a 50% fill level . As is evident in the images of segregation patterns, darker areas correspond to the region where steel beads are dominant and lighter areas correspond to where glass beads are dominant. Quantitative image analysis is performed to study: (i) degree of segregation; and (ii) shape of the segregated pattern. The degree of segregation is measured as a function of area occupied by the segregated pattern. We define the "segregation index" analogous to that used for axial banding [28]. For the two-dimensional geometry, the segregation index is:

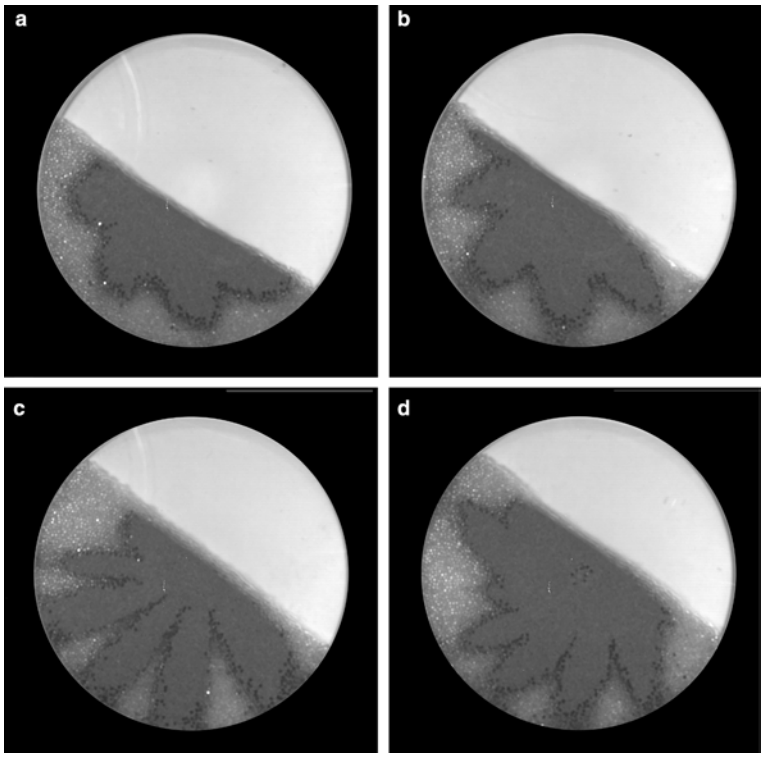

Fig. 10 Effect of fill level on granular segregation. Segregation patterns after 20 rotations 1 mm steel beads and 3 mm glass beads ($d_s/d_g = 0.33$) (a) 40% fill level (b) 48% fill level; (c) 60% fill level; and (d) 65% fill level. 50% fill level is shown in Fig. 4b

$$\sigma = \frac{\left[A(\frac{\pi}{8}D^2 - A)\right]^{1/2}}{\frac{\pi}{8}D^2} \quad (1)$$

where, A is the area occupied by one bead type and ($\pi D^2/8 - A$) is the remaining area occupied by the other bead type. Therefore, segregation index is the geometric mean of the area occupied by the steel and glass beads and normalized by the total area of the granular material. For perfect segregation, the core area (A) should be one-quarter of the total area of the tumbler. For this case, the segregation index (σ) will be 0.5. A core area that is smaller or larger than theoretical area for maximum segregation would suggest more mixing or poorer segregation. For example, a core that occupies 5% or 95% of the total filled area has a segregation index of $\sigma = 0.22$. For no segregation (the core occupies 0% or 100% of the total filled area), $\sigma = 0$.

The shape of the segregated section is quantified as a "shape index" (p^2/A), as used by Hill et al. [30], where p is the perimeter of segregated pattern and A is the area occupied by it. For the case of "*classical*" radial segregation (semi-circular core) of radius r, the perimeter of the pattern (p) is $(2 + \pi)\, r$ while the area of the pattern (A) is $\pi r^2/2$. Therefore, the value of $p^2/A = (2 + \pi)^2\ (2/\pi) \sim 17$, which happens to be the minimum value of p^2/A. Deviations from "classical" core result in a much larger value of the perimeter and hence, a value for p^2/A much larger than 17.

Figure 11a shows the dependence of both the segregation index (σ) and shape index (p^2/A) on the number of rotations (N) for 4 mm glass and steel beads (a classical core situation). Based on the segregation index, radial segregation is quite fast, less than 2 rotations, and then remains nearly constant, suggesting that steady state segregation is achieved within the first few rotations. The value of segregation index is about 0.45 indicating that segregation is nearly perfect for this case. The shape index also indicates that the segregation pattern does not evolve after the initial formation of the core. The shape index is slightly less than 30. The reason this value is significantly higher than the theoretical value of 17 for semi-circular core is the granularity of the core boundary resulting in a perimeter greater than that for a perfect semi-circle. Figure 11b shows the same measurements for 1 mm steel and 2 mm glass beads, a case for which streaks form. In this case, the shape index starts out at a value near 25, similar to that for a classical core. However, the shape index increases with time eventually reaching a value averaging 64 after about 10 rotations. For all the cases in which radial streaks occur, segregation starts as a semi-circular core and later evolves into radial streaks. Beyond 10 rotations, there are no changes in the segregation pattern. The oscillatory variation of the shape index between 60 and 75 after 10 revolutions comes about as individual streaks enter and leave the flowing layer. The segregation index (σ) reaches a value of around 0.45 within two rotations. Then the segregation index decreases slightly from 2 to 10 rotations suggesting that the segregation is not quite as complete as the core changes into radial streaks. Beyond 10 rotations, segregation index remains essentially constant.

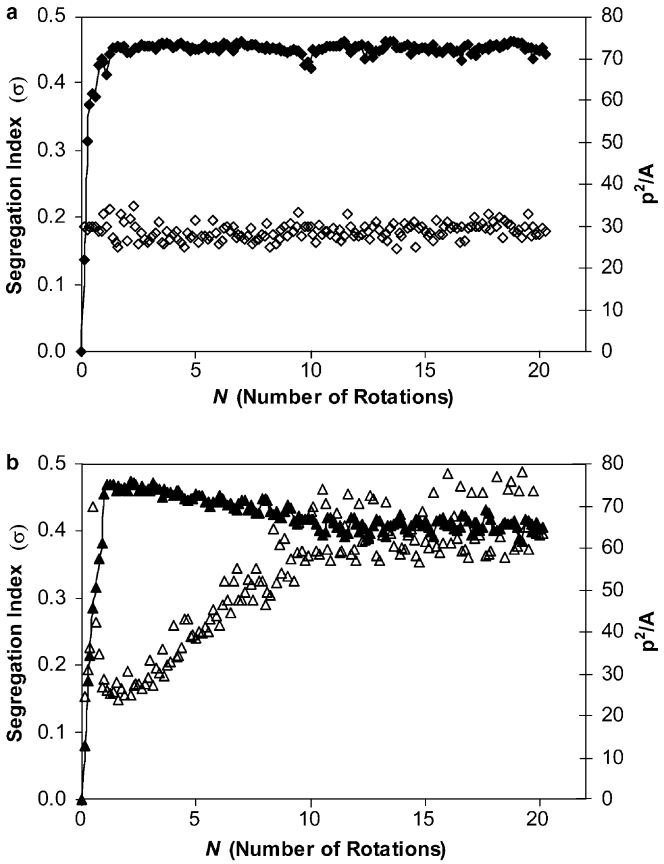

Fig. 11 Dependence of the segregation index (σ) and shape index (p^2/A) on the number of rotations (N). (a) 4 mm steel and 4 mm glass beads ($d_s/d_g = 1$); (b) 1 mm steel and 2 mm glass beads ($d_s/d_g = 0.5$). Symbol fill: open, shape index (p^2/A); black, segregation index (σ)

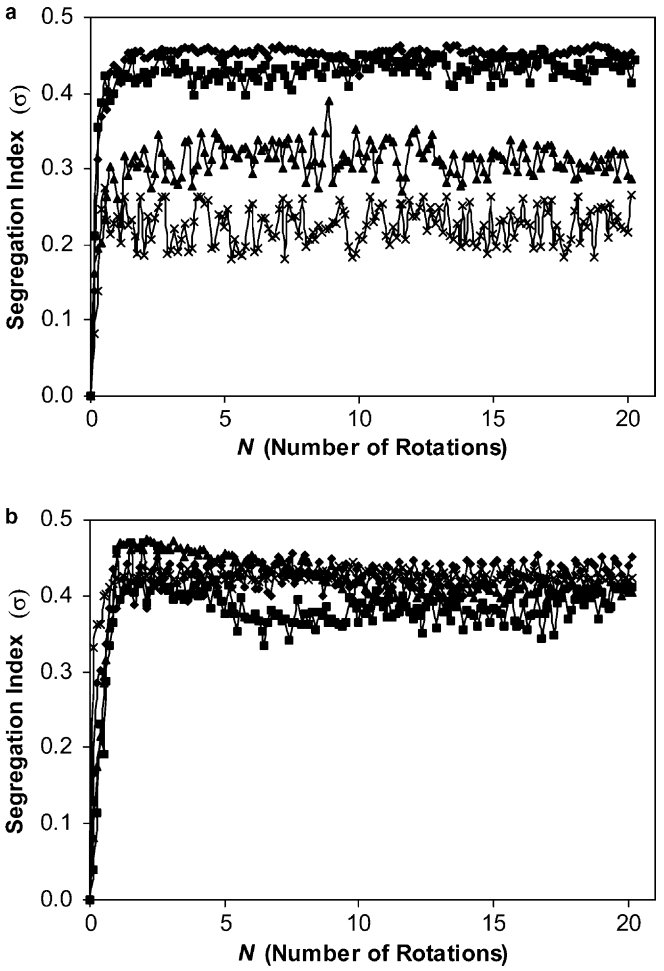

Fig. 12 Dependence of the segregation index (σ) on the number of rotations (N). (a) "S−D" system - 4 mm steel beads tumbled with 1 mm, 2 mm, 3 mm, and 4 mm glass beads ($d_s/d_g = 4$, 2, 1.33, and 1.0); (b) "S+D" system - 1 mm steel beads tumbled with 1 mm, 2 mm, 3 mm, and 4 mm glass beads ($d_s/d_g = 1.0$, 0.5, 0.33, and 0.25). Symbols: ×, $d_g = 1$ mm; ▲, $d_g = 2$ mm; ■, $d_g = 3$ mm; ♦, $d_g = 4$ mm

Figure 12a shows the segregation index for 4 mm steel beads with 1, 2, 3, and 4 mm glass beads. The segregation index is highest for 3 and 4 mm glass beads where a classical core of more dense beads forms. The segregation index decreases as the size of glass beads decreases to 2 mm (a small glass bead core surrounded by a band of steel beads, and a band of glass beads at the periphery). For the case of 4 mm steel and 1 mm glass beads, where only a concentrated band of steel beads forms at the periphery, the segregation index drops down to a value close to 0.2 suggesting poor segregation. For the case of 4 mm steel beads and 0.2 mm glass beads (not shown in Fig. 12a), $\sigma = 0$ indicating mixed beads. Figure 12b shows the segregation index for 1 mm steel beads and with beads of diameter 1, 2, 3, and 4 mm. The segregation index in all these cases is around 0.40 suggesting relatively strong segregation, consistent with buoyancy and percolation acting together. For the cases where a classical core forms (1 mm steel beads with 1 mm or 4 mm glass beads), the segregation index remains flat after a few rotations. However, for the cases where streaks form (1 mm steel beads with 2 or 3 mm glass beads), the segregation index has a slight transient for the first 5 to 10 rotations as streaks form.

4 Conclusions

At this point it is possible to answer some of the questions posed in the introduction: What size and density combinations result in mixing? When does percolation dominate over buoyancy, and vice versa? How do the segregation patterns depend on the type of particles?

Consider first when mixing occurs. Figure 8 and Fig. 12a indicate that segregation is reduced when $d_s/d_g > 2$ and mixing occurs for $10 \leq d_s/d_g \leq 20$. Of course, these experiments are limited to only two different types of particles with a density ratio of approximately 3. However, additional insight can be gained from considering our results along with results of Drahun and Bridgwater [25], Alonso et al. [26], and Metcalfe and Shattuck [27]. The size and density ratios corresponding to the situations where segregation is nearly eliminated are shown in Table 1 for the experimental configurations used in these studies. These ratios of particle

Table 1 Size and density ratio at which percolation and buoyancy offset each other

ρ_{heavy} (g/cm^3)	$\rho_{heavy}/\rho_{light}$	d_{heavy}/d_{light}	Type of material	Type of flow	Reference
2.5	2.3	1.3	Glass Beads/Tracer	Free surface flow	[25]
7.8	3.1	2.2	Steel Beads/Glass Beads	Rolling regime – rotating tumbler	[26]
2.5	2.5	1.6	Glass Beads/Plastic Beads	Rolling regime – rotating tumbler	[26]
2.5	1.4	1.4	Glass Beads/Mustard Seeds	Avalanching regime – rotating tumbler	[27]
7.5	3	> 2	Steel Beads/Glass Beads	Rolling regime – rotating tumbler	Current Study

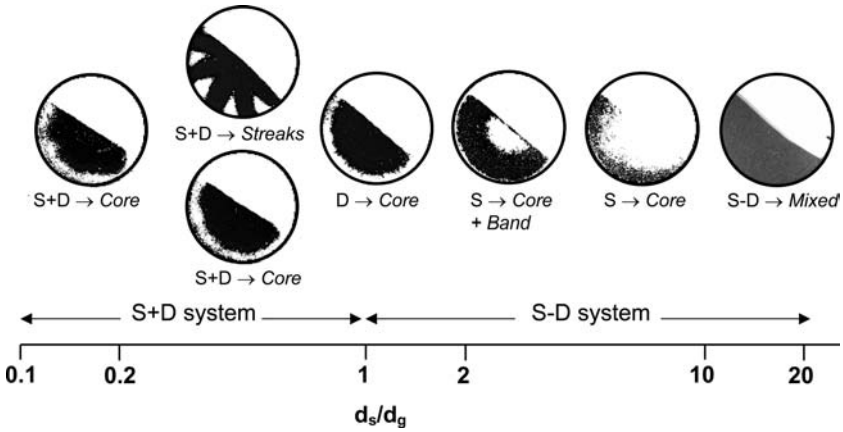

Fig. 13 Dependence of segregation regimes on the ratio (d_s/d_g). For $d_s/d_g \leq 1$, steel beads are located either in a semi-circular core or in radial streaks. For $1 < d_s/d_g < 10$, glass beads are in the core and, in some cases, at the periphery. For $d_s/d_g \geq 10$, mixing occurs

size and particle density at which segregation is minimized are not precise. They depend on the method that was used to determine and measure segregation and other experimental parameters. Nevertheless, even though the nature of the granular flows is somewhat different (avalanching vs. rolling regime, free surface flow vs. flow in a tumbler, 50% fill vs. 75% fill, two-dimensional vs. three-dimensional tumbler), it appears that segregation is eliminated when d_{heavy}/d_{light} and $\rho_{heavy}/\rho_{light}$ have similar values. Furthermore, mixing improves as the ratio d_{heavy}/d_{light} becomes substantially larger than $\rho_{heavy}/\rho_{light}$, and segregation dominates when d_{heavy}/d_{light} is less than $\rho_{heavy}/\rho_{light}$ (this relationship is valid only for SD-systems and not for S- or D-systems). Since the particle mass is directly related to the particle diameter and density, this relation can be recast in terms of the mass of the particles, m, so that mixing dominates when $d_{heavy}/d_{light} > (m_{heavy}/m_{light})^{1/4}$.

The question of whether density or particle size are the dominant segregation mechanism can be answered by considering the beads that form the core. If the core is composed of denser beads, then segregation is dominated by buoyancy (density); if the core is composed of smaller beads, then segregation is dominated by percolation (size). For the particle sizes and densities investigated here, percolation dominates in most of the cases. When the steel beads are smaller than the glass beads so that buoyancy and percolation act in the same direction, streaks form because of differences in particle "fluidity". Conversely, when the steel beads are larger than the glass beads so that buoyancy and percolation oppose one another, heavy beads form a core in only one case (4 mm steel beads and 3 mm glass beads, $d_s/d_g = 1.33$). For all other cases, smaller glass beads form the core, with larger steel beads near the periphery of the tumbler.

A summary of the dependence of the results on the size ratio, d_s/d_g, is shown in Fig. 13. A "classical" core is formed when the particles are of the same size but differ in density ($d_s/d_g = 1$). When the heavier beads are smaller than the lighter beads ($d_s/d_g < 1$), deviations from the "classical" core pattern can occur in some cases in the form of radial streaks. These streaks are formed because of the differences in "fluidity" of the particles. In other cases at similar size ratios (for example at $d_s/d_g = 0.5$), a traditional core forms. The streaks disappear completely if the particle sizes are very different from each other ($d_s/d_g \ll 1$). When the heavier beads are slightly larger that the lighter beads ($d_s/d_g \approx 2$), percolation and buoyancy oppose one another resulting in a small core of small beads, a band of large beads, and a narrow band of small beads at the periphery. Apparently, percolation causes the formation of a small core of small beads, while buoyancy causes some small beads to remain at the periphery of the tumbler. Increasing the size ratio causes percolation to dominate so that the core of small beads is larger and the band of small beads at the periphery disappears. Mixing occurs only when the heavy particles are substantially larger than the light particles ($d_s/d_g \gg 1$). This is a very important practical result. If it is necessary to mix particles of different densities, it is best to use large particles of the more dense material and small particles of the less dense material.

The work described here raises several issues for further research. Current theoretical models for segregation

are limited to either S-systems or D-systems. A combined model that accounts for the interaction between size and density would be useful. However, the model would need to account for "fluidity" of the granular material, an aspect that needs more investigation and quantification. Finally, using a non-circular tumbler introduces complexity that results from the interaction between segregation and chaotic advection. While the previous work of Hill et al. [30] was limited to either S- or D-systems, the SD-system in a non-circular tumbler may be even more complex because of additional competition between different segregation mechanisms on top of the competition between chaos and segregation.

Acknowledgements This work was funded by the Office of Basic Energy Sciences of the Department of Energy. We thank Nick Pohlman for his help in the design of experimental apparatus. Nitin Jain acknowledges the support of his employer ZS Associates.

References

1. Lacey, P.M.: J. Appl. Chem. **4**, 257 (1954)
2. Williams, J.C.: Fuel Soc. J. **14**, 29 (1963)
3. Bridgwater, J.: Powder Technol. **15**, 215 (1976)
4. Jaegar, H.M., Nagel, S.R.: Science **255**, 1523 (1992)
5. Ristow, G.H.: Pattern formation in granular materials. (Springer, 2000)
6. Duran, J.: Sands, Powders, and Grains. (Springer Publication, 2000)
7. Ottino, J.M., Khakhar, D.V.: Ann. Rev. Fluid Mech. **32**, 55 (2000)
8. Ottino, J.M.: The kinematics of mixing: stretching, chaos and transport. (Cambridge, UK: Cambridge University Press, 1989)
9. Rosato, A., Strandburg, K.J., Prinz, F., Swendsen, R.H.: Phys. Rev. Lett. **58**, 1038 (1987)
10. Thomas, N.: Phys. Rev. E **62**, 961 (2000)
11. Huerta, D., Ruiz-Suárez, J.: Phys. Rev. Lett. **92**, 114301 (2004)
12. Shinbrot, T., Muzzio, F.J.: Phys. Rev. Lett. **81**, 4365 (1998)
13. Khakhar, D.V., McCarthy, J.J., Ottino, J.M.: Chaos **9**, 594 (1999)
14. Rajchenbach, J.: Phys. Rev. Lett. **65**, 2221 (1990)
15. Henein, H., Brimacomble, J.K., Watkinson, A.P.: Metal. Trans. B **14**, 191 (1983)
16. Donald, M.B., Roseman, B.: Br. Chem. Eng. **7**, 749 (1962)
17. Nityanand, N., Manley, B., Henein, H.: Metal. Trans. B **17**, 247 (1986)
18. Clement, E., Rajchenbach, J., Duran, J.: Europhys. Lett. **30**, 7 (1995)
19. Cantalaube, F., Bideau, D.: Europhys. Lett. **30**, 133 (1995)
20. Khakhar, D.V., McCarthy, J.J., Ottino, J.M.: Phys. Fluids **9**, 3600 (1997)
21. Khakhar, D.V., Orpe, A.V., Ottino, J.M.: Powder Technol. **116**, 232 (2001)
22. Ristow, G.H.: Europhys. Lett. **28**, 97 (1994)
23. Dury, C.M., Ristow, G.H.: J. Phys. I France **7**, 737 (1997)
24. Prigozhin, L., Kalman, H.: Phys. Rev. E **57**, 2073 (1998)
25. Drahun, J.A., Bridgwater, J.: Powder Technol. **36**, 39 (1983)
26. Alonso, M., Satoh, M., Miyanami, K.: Powder Technol. **68**, 145 (1991)
27. Metcalfe, G., Shattuck, M.: Physica A. **233**, 709 (1996)
28. Jain, N., Khakhar, D.V., Lueptow, R.M., Ottino, J.M.: Phys. Rev. Lett. **86**, 3771 (2001)
29. Hill, K.M., Kakalios, J.: Phys. Rev. E **49**, 3610 (1994)
30. Hill, K.M., Khakhar, D.V., Gilchrist, J. F., McCarthy, J.J., Ottino, J.M.: P. Natl. Acad. Sci. USA **96**, 11701 (1999)
31. Jain, N., Ottino, J.M., Lueptow, R.M.: J. Fluid Mech. 508, 23 (2004)
32. Jain, N., Ottino, J.M., Lueptow, R.M.: Phys. Fluids **14**, 572 (2002)